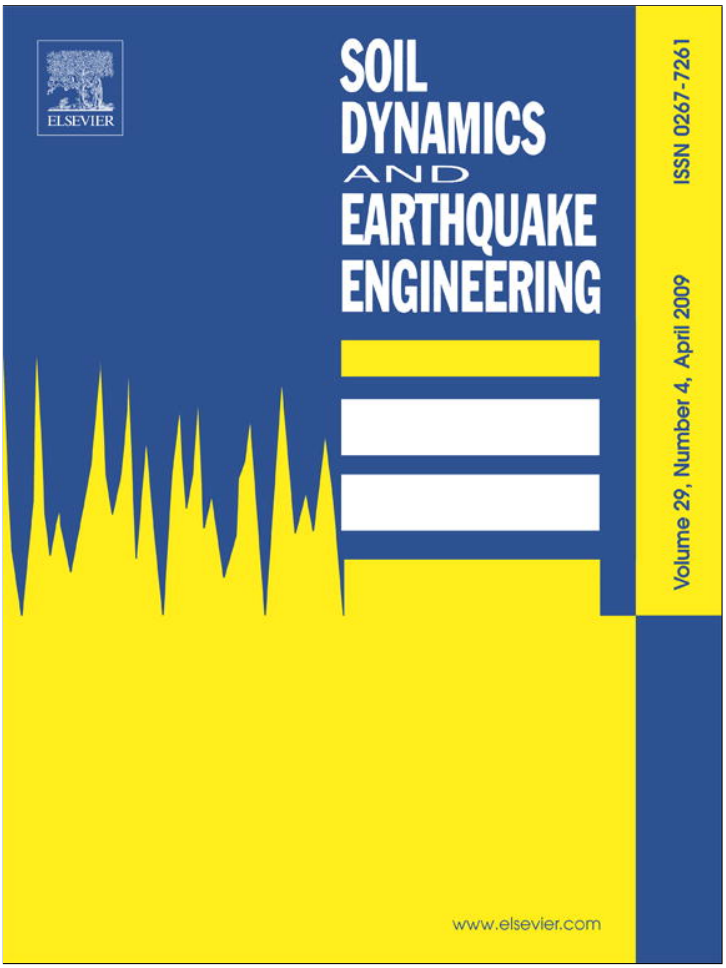

Soil Dynamics and Earthquake Engineering 29 (2009) 658–668

Contents lists available at ScienceDirect

Soil Dynamics and Earthquake Engineering

journal homepage: www.elsevier.com/locate/soildyn

Seismic response of base-isolated buildings including soil–structure interaction

C.C. Spyrakos *, I.A. Koutromanos, Ch.A. Maniatakis

Laboratory for Earthquake Engineering, School of Civil Engineering, National Technical University of Athens, Zografos, Athens 15700, Greece

ARTICLE INFO

Article history:
Received 5 October 2006
Received in revised form
3 July 2008
Accepted 5 July 2008

Keywords:
Soil–structure interaction
Building structures
Base isolation
Seismic response

ABSTRACT

This study investigates the effect of soil–structure interaction (SSI) on the response of base-isolated buildings. The equations of motion are formulated in the frequency domain, assuming frequency-independent soil stiffness and damping constants. An equivalent fixed-base system is developed that accounts for soil compliance and damping characteristics of the base-isolated building. Closed-form expressions are derived, followed by a thorough parametric study involving the pertinent system parameters. For preliminary design, the methodology can serve as a means to assess effective use of base isolation on building structures accounting for SSI. This study concludes that the effects of SSI are more pronounced on the modal properties of the system, especially for the case of squat and stiff base-isolated structures.

1. Introduction

Use of base isolation is increasingly applied to seismically upgrade existing buildings as well as to effectively reduce the seismic vulnerability of new buildings. It is also well recognized that soil–structure interaction (SSI) could play a significant role on structural response. However, common practice usually does not account for the effects of SSI on the seismic behaviour of base-isolated structures. The present study attempts to quantify the effects of SSI on base-isolated building structures.

The effects of SSI on the seismic response of structures had not been seriously taken into account until the 1971 San Fernando earthquake and the beginning of nuclear plant construction in the earthquake-prone California. The substantial number of journal papers, e.g., Wong and Luco [1], and design guides, e.g., Idriss et al. [2] published in the 1970s, reflect the great importance of the phenomenon.

In the 1980s and 1990s, SSI was studied thoroughly thanks to the impressive development of numerical methods, e.g., Spyrakos and Beskos [3], Gazetas [4] and Wolf [5,6]. Also, many studies investigated the effects of SSI on special structures, e.g., Goyal and Chopra [7], Xu and Spyrakos [8], Maekawa et al. [9]. A detailed discussion on SSI effects and analysis techniques is presented by Johnson [10]. The inclusion of SSI phenomena in the seismic analysis and design of structures is addressed in seismic code provisions, including the recent FEMA 450 document [11]. Simple criteria have been developed in order to decide whether SSI effects must be taken into account and, if so, the degree that the building eigenperiods and damping vary with specific dimensionless system parameters, e.g., Spyrakos [12].

The modification of seismic structural response through application of base isolation has been the subject of extensive research for the last 25 years, mainly in the United States, Europe and Japan [13–15]. Despite the fact that in most cases isolation devices behave nonlinearly, it is common practice to use a linear analysis for the seismic design of most base-isolated structures [16]. The spread of base isolation has been assisted by the development of appropriate design codes for isolated structures. Commonly applied codes, such as the International Building Code 2000 [17] and Eurocode 8 [18], address most of the practical issues regarding concepts and procedures related to base isolation.

Several studies have been made to assess the effect of SSI phenomena on the seismic response of base-isolated bridges. Chaudhary et al. [19] have identified the structural and geotechnical parameters of four base-isolated bridges using available theoretical models and data from recent earthquakes. The main conclusions of their study are that SSI effects depend primarily on horizontal pier stiffness in relation to the soil horizontal stiffness, and that the important reduction in the soil shear modulus for moderate earthquakes should be definitely incorporated into SSI analyses. Spyrakos and Vlassis [20] and Vlassis and Spyrakos [21] performed analytical studies of SSI effects on the longitudinal response of base-isolated bridge piers concerning the increase in damping and the decrease in base shear, as calculated by contemporary bridge design codes. They reached the conclusion that SSI causes a significant decrease in the system

* Corresponding author. Tel.: +30 2107721187; fax: +30 2107721182.
E-mail address: spyrakos@hol.gr (C.C. Spyrakos).

0267-7261/$ - see front matter © 2008 Elsevier Ltd. All rights reserved.
doi:10.1016/j.soildyn.2008.07.002

eigenfrequencies and a rather insignificant increase in the system damping that is dominated by the isolation system damping ratios.

Sarrazin et al. [22] presented the response of base-isolated bridges for ambient vibration tests and earthquake excitations in Chile. They reported differences between the Fourier amplitude spectra of the numerical analyses that they performed and the earthquake recordings, which may be attributed to SSI effects. Iemura and Pradono [23] numerically evaluated the effectiveness of passive isolators and semi-active dampers on an existing cable-stayed bridge. Since the bridge towers were founded on a soft 35 m-thick soil layer, SSI was taken into account. It was found that the flexibility introduced by the soil reduced the dampers deformation and, in consequence, the amount of damping in the retrofitted bridge. Tongaonkar and Jangid [24] presented the SSI effects on a three-span bridge with LRBs, assuming frequency-independent expressions for the soil stiffness and damping parameters. Their numerical study revealed an increase in the seismic displacements when SSI is included, a fact that should be taken into account for the design of bridges.

Cho et al. [25] and Kim et al. [26] investigated the seismic response of base-isolated liquid storage tanks, accounting for the effects of fluid–structure–soil interaction. They performed a series of numerical analyses using a coupled finite element—boundary element formulation in the time domain. Their study revealed that soil flexibility results in smaller displacement and force amplitudes, but leaves the contained fluid motion unaffected.

According to the authors' knowledge, very little has been made on the investigation of SSI effects on base-isolated buildings, such as the work by Constantinou and Kneifati [27] and Tsai et al. [28]. Constantinou and Kneifati [27] have investigated the effect of SSI on the dynamic characteristics of a base-isolated structure. They have also examined the ability of a simple energy-based method to yield results of satisfactory accuracy. Furthermore, Tsai et al. [28] propose that the soil compliance and damping should be taken into account for the analysis of base-isolated buildings. Their findings are based on numerical analyses of FPS-isolated buildings, and revealed that SSI results in larger displacement and, in some sections in the structure, larger shear forces.

This study presents a methodology to assess the effect of SSI on base-isolated building structures, such as the one shown in Fig. 1. A simplified model is developed in which the building, its foundation, the base isolation and the soil are studied as a four-degree-of-freedom (4-DOF) system. The methodology could serve as a means to perform a preliminary analysis in order to evaluate the effectiveness of base isolation in conjunction with SSI.

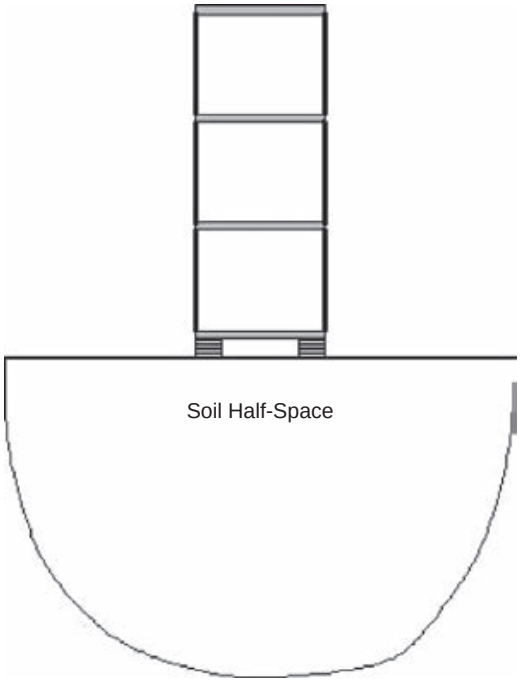

Fig. 1. Base-isolated structure found on soil half-space.

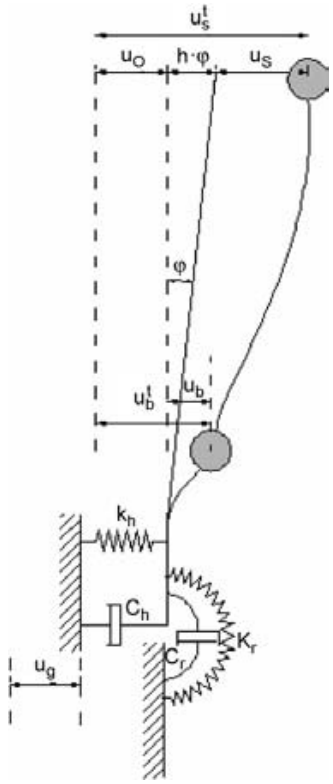

Fig. 2. Analytical model for base-isolated structure including soil impedances.

2. Analytical methodology

2.1. Equations of motion

The simplified model of the foundation–isolation-structure system is shown in Fig. 2. With reference to Fig. 2, it can be deduced that the relative with respect to the ground motion displacements are expressed as

$$u_s^t = u_o + h\varphi + u_s \tag{1a}$$

$$u_b^t = u_o + u_b \tag{1b}$$

In order to obtain the equations of motion of the system, Lagrange's equations are employed, that is

$$\frac{d}{dt}\left(\frac{\partial K}{\partial \dot{q}_i}\right) - \frac{\partial K}{\partial q_i} + \frac{\partial U}{\partial q_i} + \frac{\partial D}{\partial \dot{q}_i} = 0 \tag{2}$$

with K, U and D denoting the kinetic, potential and dissipation energy, respectively, $q_i(t)$ are the degrees-of-freedom of the system and dot denotes differentiation with respect to time. With appropriate manipulations, Eq. (2) yields the following

equations of motion in matrix form:

$$\begin{bmatrix} m_s & 0 & m_s & m_s h \\ 0 & m_b & m_b & 0 \\ m_s & m_b & m_s+m_b & m_s h \\ m_s h & 0 & m_s h & m_s h^2 \end{bmatrix} \begin{Bmatrix} \ddot{u}_s \\ \ddot{u}_b \\ \ddot{u}_o \\ \ddot{\varphi} \end{Bmatrix} + \begin{bmatrix} c_s & -c_s & 0 & 0 \\ -c_s & c_b+c_s & 0 & 0 \\ 0 & 0 & c_h & 0 \\ 0 & 0 & 0 & c_r \end{bmatrix} \begin{Bmatrix} \dot{u}_s \\ \dot{u}_b \\ \dot{u}_o \\ \dot{\varphi} \end{Bmatrix} + \begin{bmatrix} k_s & -k_s & 0 & 0 \\ -k_s & k_b+k_s & 0 & 0 \\ 0 & 0 & k_h & 0 \\ 0 & 0 & 0 & k_r \end{bmatrix} \begin{Bmatrix} u_s \\ u_b \\ u_o \\ \varphi \end{Bmatrix} = -\begin{Bmatrix} m_s \\ m_b \\ m_s+m_b \\ m_s h \end{Bmatrix} \ddot{u}_g \tag{3}$$

where k_s, k_b, k_r and k_h are the stiffness coefficients corresponding to the structural, isolation and foundation rotational and horizontal degree-of-freedom, respectively; c_s, c_b, c_r and c_h are the viscous damping coefficients corresponding to the structural, isolation and foundation rotational and horizontal degree-of-freedom, respectively; m_s and m_b the mass coefficients corresponding to the structural and isolation degree-of-freedom, respectively, and $\ddot{u}_g$ is the ground motion acceleration. The parameter h denotes the equivalent structural height, defined as the height of an equivalent single degree-of-freedom (SDOF) system. Usually, h is taken as equal to the structural height for single-storey buildings, while for multi-storey buildings it can be approximately set as equal to 0.7 times the total height of the building or be calculated with an appropriate expression, e.g., Priestley [29].

The following parameters are introduced:

$$\omega_h^2 = \frac{k_h}{m_b+m_s}, \quad \omega_r^2 = \frac{k_r}{m_s h^2}, \quad \omega_s^2 = \frac{k_s}{m_s}, \quad \omega_b^2 = \frac{k_b}{m_b+m_s} \tag{4}$$

$$\zeta_s = \frac{\omega c_s}{2k_s}, \quad \zeta_b = \frac{\omega c_b}{2k_b}, \quad \zeta_h = \frac{\omega c_h}{2k_h}, \quad \zeta_r = \frac{\omega c_r}{2k_r} \tag{5}$$

By assuming a harmonic base excitation, $u_g = e^{i\omega t}$ and performing several algebraic manipulations, Eq. (3) transforms to the following set of equations:

$$-m_s\omega^2(u_s+u_o+h\varphi) + k_s(1+2\zeta_s i)(u_s-u_b) = m_s\omega^2 u_g \tag{6a}$$

$$-m_b\omega^2(u_b+u_o) + k_b(1+2\zeta_b i)u_b - k_s(1+2\zeta_s i)(u_s-u_b) = m_b\omega^2 u_g \tag{6b}$$

$$-m_b\omega^2(u_b+u_o) - m_s\omega^2(u_s+u_o+h\varphi) + k_h(1+2\zeta_h i+2\zeta_g i)u_o = (m_b+m_s)\omega^2 u_g \tag{6c}$$

$$-m_s h\omega^2(u_s+u_o+h\varphi) + k_r(1+2\zeta_r i+2\zeta_g i)\varphi = m_s h^2\omega^2 u_g \tag{6d}$$

Using Eqs. (4)–(5), Eqs. (6a)–(6d) can be expressed as

$$(\beta_1-1)u_s - \beta_1 u_b - u_o - h\varphi = u_g \tag{7a}$$

$$-[\gamma\beta_1]u_s + \left[-(1-\gamma)+\frac{\omega_b^2}{\omega^2}\beta_2+\gamma\beta_1\right]u_b - (1-\gamma)u_o = (1-\gamma)u_g \tag{7b}$$

$$-\gamma u_s - (1-\gamma)u_b + (-1+\beta_3)u_o - \gamma u_o = u_g \tag{7c}$$

$$-u_s - u_b + (-1+\beta_4)h\varphi = u_g \tag{7d}$$

where the mass ratio γ and the parameters β_1, β_2, β_3 and β_4 are defined as

$$\gamma = \frac{m_s}{m_s+m_b} \tag{8}$$

$$\beta_1 = \frac{\omega_s^2}{\omega^2}(1+2\zeta_s i) \tag{9}$$

$$\beta_2 = \frac{\omega_b^2}{\omega^2}(1+2\zeta_b i) \tag{10}$$

$$\beta_3 = \frac{\omega_h^2}{\omega^2}(1+2\zeta_h i+2\zeta_g i) \tag{11}$$

$$\beta_4 = \frac{\omega_r^2}{\omega^2}(1+2\zeta_r i+2\zeta_g i) \tag{12}$$

Since the system consists of a massless foundation, only two degree-of-freedom (2-DOF) can be considered as dynamic; namely, the structural, u_s and the isolation, u_b. As presented in Part I of Appendix A, the equations of motion can be expressed with reference to an equivalent 2-DOF system, that contains the structural and the isolation degrees-of-freedom, that is

$$([\tilde{K}]+i[\tilde{\zeta}])\begin{Bmatrix} u_s \\ u_b \end{Bmatrix} = \begin{Bmatrix} \dfrac{\omega^2}{\tilde{\omega}_s^2} \\ (1-\gamma)\dfrac{\omega^2}{\tilde{\omega}_b^2} \end{Bmatrix} \tilde{u}_g \tag{13}$$

where the complex stiffness matrix of the equivalent 2-DOF system is given by

$$([\tilde{K}]+i[\tilde{\zeta}]) = \begin{bmatrix} 1+2\tilde{\zeta}_s i-\dfrac{\omega^2}{\tilde{\omega}_s^2} & -(1+2\tilde{\zeta}_s i) \\ -\dfrac{\tilde{\omega}_s^2}{\tilde{\omega}_b^2}\gamma(1+2\tilde{\zeta}_s i) & 1+2\tilde{\zeta}_b i+\dfrac{\tilde{\omega}_s^2}{\tilde{\omega}_b^2}\gamma(1+2\tilde{\zeta}_s i)-(1-\gamma)\dfrac{\omega^2}{\tilde{\omega}_b^2} \end{bmatrix} \tag{14}$$

2.2. Modal properties

The eigenfrequencies of the equivalent 2-DOF system can be calculated from Eqs. (13) and (14) by setting $\tilde{\zeta}_b = \tilde{\zeta}_s = 0$, that is

$$\begin{bmatrix} 1-\dfrac{\omega^2}{\tilde{\omega}_s^2} & -1 \\ -\dfrac{\tilde{\omega}_s^2}{\tilde{\omega}_b^2}\gamma & 1+\dfrac{\tilde{\omega}_s^2}{\tilde{\omega}_b^2}\gamma-(1-\gamma)\dfrac{\omega^2}{\tilde{\omega}_b^2} \end{bmatrix} \{\tilde{\Phi}^m\} = 0, \quad m = 1,2 \tag{15}$$

The eigenfrequencies of the equivalent 2-DOF system can be expressed as

$$\tilde{\omega}_{1,2}^2 = \frac{(1+\tilde{R}_s\gamma) \mp \sqrt{(1+\tilde{R}_s\gamma)^2 - 4(1-\gamma)\tilde{R}_s\gamma}}{2(1-\gamma)}\tilde{\omega}_s^2 \tag{16}$$

where $\tilde{R}_s = \tilde{k}_b/\tilde{k}_s$ is the equivalent system stiffness ratio.

The two modes can be determined from Eq. (15) and are given by

$$\{\tilde{\Phi}^1\} = \begin{Bmatrix} 1 \\ 1-\tilde{\alpha}_1 \end{Bmatrix}, \tag{17a}$$

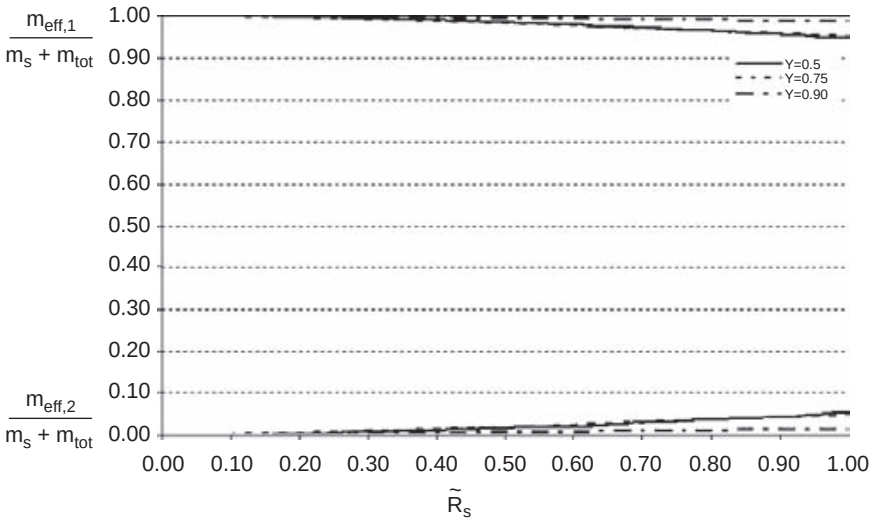

Fig. 3. Effective modal mass ratios for the first (isolation) and second (structural) mode of the equivalent 2-DOF system.

$$\{\tilde{\Phi}^2\} = \begin{Bmatrix} 1 \\ 1-\tilde{\alpha}_2 \end{Bmatrix}, \tag{17b}$$

in which

$$\tilde{\alpha}_1 = \frac{\tilde{\omega}_1^2}{\tilde{\omega}_s^2} \tag{18a}$$

$$\tilde{\alpha}_2 = \frac{\tilde{\omega}_2^2}{\tilde{\omega}_s^2} \tag{18b}$$

$\{\tilde{\Phi}^1\}$ and $\{\tilde{\Phi}^2\}$ are called the isolation and structural modes, respectively. The effective modal mass ratios, that is the effective modal mass over the total mass of the system, are given by

$$\begin{aligned}\frac{m_{\text{eff},1}}{m_b+m_s} &= \frac{1}{m_b+m_s}\frac{(\{\tilde{\Phi}^1\}^T[\tilde{M}]\{r\})^2}{\{\tilde{\Phi}^1\}^T[\tilde{M}]\{\tilde{\Phi}^1\}} \\ &= \frac{1}{m_b+m_s}\frac{\left(\begin{bmatrix}1 & 1-\tilde{\alpha}_1\end{bmatrix}\begin{bmatrix}m_b & 0\\ 0 & m_s\end{bmatrix}\begin{Bmatrix}1\\1\end{Bmatrix}\right)^2}{\begin{bmatrix}1 & 1-\tilde{\alpha}_1\end{bmatrix}\begin{bmatrix}m_b & 0\\ 0 & m_s\end{bmatrix}\begin{Bmatrix}1\\1-\tilde{\alpha}_1\end{Bmatrix}} \\ &= \frac{1}{m_b+m_s}\frac{[(1-\gamma)+(1-\tilde{\alpha}_1)\gamma]^2}{(1-\gamma)+(1-\tilde{\alpha}_1)^2\gamma}(m_b+m_s) \\ &= \frac{[(1-\gamma)+(1-\tilde{\alpha}_1)\gamma]^2}{(1-\gamma)+(1-\tilde{\alpha}_1)^2\gamma}\end{aligned} \tag{19}$$

$$\begin{aligned}\frac{m_{\text{eff},2}}{m_b+m_s} &= \frac{1}{m_b+m_s}\frac{(\{\tilde{\Phi}^2\}^T[\tilde{M}]\{r\})^2}{\{\tilde{\Phi}^2\}^T[\tilde{M}]\{\tilde{\Phi}^2\}} \\ &= \frac{1}{m_b+m_s}\frac{\left(\begin{bmatrix}1 & 1-\tilde{\alpha}_2\end{bmatrix}\begin{bmatrix}m_b & 0\\ 0 & m_s\end{bmatrix}\begin{Bmatrix}1\\1\end{Bmatrix}\right)^2}{\begin{bmatrix}1 & 1-\tilde{\alpha}_2\end{bmatrix}\begin{bmatrix}m_b & 0\\ 0 & m_s\end{bmatrix}\begin{Bmatrix}1\\1-\tilde{\alpha}_2\end{Bmatrix}} \\ &= \frac{1}{m_b+m_s}\frac{[(1-\gamma)+(1-\tilde{\alpha}_2)\gamma]^2}{(1-\gamma)+(1-\tilde{\alpha}_2)^2\gamma}(m_b+m_s) \\ &= \frac{[(1-\gamma)+(1-\tilde{\alpha}_2)\gamma]^2}{(1-\gamma)+(1-\tilde{\alpha}_2)^2\gamma}\end{aligned} \tag{20}$$

The variation of the effective mass rations with respect to the stiffness ratio $\tilde{R}_s$ is depicted in Fig. 3. It can be deduced that the effective mass ratio of the first mode is greater than 90% for the range of $\tilde{R}_s$ values examined. Thus, the contribution of the second mode is negligible compared with that of the fundamental mode. Therefore, it is justifiable to consider that the modal viscous damping ratio of the first mode describes the behaviour of the system adequately.

2.3. Damping ratios of equivalent system

The relations between the equivalent 2-DOF system parameters $\tilde{\omega}_b$ band $\tilde{\omega}_s$ with the corresponding parameters of the 4-DOF system, as elaborated in Part II of Appendix A, can be obtained by imposing that the coefficients of u_s and u_b in the undamped formulation of the two systems are equal, that is

$$\frac{\tilde{\omega}_b^2}{\omega_b^2} = \frac{\omega_r^2}{\omega_b^2+\omega_r^2} \tag{21}$$

$$\frac{\tilde{\omega}_s^2}{\omega_s^2} = \frac{\omega_r^2}{\omega_s^2+\omega_r^2} \tag{22}$$

The terms of the matrix $[\tilde{\zeta}]$ of the equivalent 2-DOF system can also be obtained by applying the same procedure for damped response as elaborated in Part II of Appendix A, to arrive at

$$[\tilde{\zeta}] = \begin{bmatrix} \tilde{\zeta}_{s11} & -\tilde{\zeta}_{s12} \\ \dfrac{-\tilde{\zeta}_{s21}}{\tilde{R}_s} & \tilde{\zeta}_{b22}+\dfrac{1}{\tilde{R}_s}\tilde{\zeta}_{s22} \end{bmatrix} \tag{23}$$

where the terms of the matrix are explicitly given by

$$\tilde{\zeta}_{s11} = \zeta_s\left(1-\frac{\omega^2}{\omega_r^2}\right)+\frac{\omega^2}{\omega_r^2}\zeta_r+\frac{\omega^2}{\omega_r^2}\zeta_g \tag{24a}$$

$$\tilde{\zeta}_{s12} = \zeta_s\left(1-\frac{\omega^2}{\omega_r^2}\right)+\frac{\omega^2}{\omega_r^2}\zeta_r+\frac{\omega^2 R_s\gamma}{\omega_r^2}\zeta_b+\frac{\omega^2 R_s\gamma}{\omega_r^2}\zeta_h \tag{24b}$$

$$\tilde{\zeta}_{s21} = \zeta_s \tag{24c}$$

$$\begin{aligned}\tilde{\zeta}_{b22}+\frac{1}{\tilde{R}_s}\tilde{\zeta}_{s22} = &\left[1-(1-\gamma)\frac{\omega^2}{\omega_h^2}\right]\zeta_b+(1-\gamma)\frac{\omega^2}{\omega_h^2}\zeta_h \\ &+(1-\gamma)\frac{\omega^2}{\omega_h^2}\zeta_g+\frac{\zeta_s}{\tilde{R}_s}\end{aligned} \tag{24d}$$

in which $R_s = k_b/k_s$ is the stiffness ratio of the 4-DOF system.

2.4. Assessment of SSI on the base-isolated system

The following dimensionless parameters are introduced in order to facilitate an investigation of the effects of SSI on base-isolated buildings:

$$\bar{s}=\frac{\omega_s h}{v_s},\quad \bar{h}=\frac{h}{\alpha},\quad \bar{m}=\frac{m_b+m_s}{\rho\alpha^3} \tag{25}$$

where $\bar{s}$ denotes a stiffness ratio expressing the relative stiffness between the structure and the soil, v_s is the soil shear wave velocity, α is a characteristic length of the foundation, e.g., for a circular foundation α is equal to its radius, and ρ is the soil mass density. The parameter $\bar{h}$ represents the geometrical form of the structure, that is, large values of $\bar{h}$ correspond to tall, slender buildings, while small values correspond to short, squat buildings. It is well established that the spring and dashpot coefficients of the soil–structure interface degrees-of-freedom depend on the frequency of the excitation [30]. In the present study, frequency-independent coefficients are employed, using the following expressions [12]:

$$k_h=\frac{8G\alpha}{2-\nu},\quad c_h=\frac{4.6\alpha^2}{2-\nu}\rho v_s \tag{26a}$$

$$k_r=\frac{8G\alpha^3}{3(1-\nu)},\quad c_r=\frac{0.4\alpha^4}{1-\nu}\rho v_s \tag{26b}$$

Substituting Eqs. (25), (26a) and (26b) in Eqs. (21) and (22) yields:

$$\frac{\tilde{\omega}_b^2}{\omega_b^2}=\frac{8}{8+R_s\bar{s}^2\gamma^2\bar{m}3(1-\nu)} \tag{27}$$

$$\frac{\tilde{\omega}_s^2}{\omega_b^2}=\frac{8}{8R_s\gamma+R_s^2\bar{s}^2\gamma^3\bar{m}3(1-\nu)} \tag{28}$$

According to the correspondence principle, the stiffness ratios R_s and $\tilde{R}_s$ are equal [20]. Based on Veletsos and Ventura [31], the approximation that the transformation that diagonalizes the stiffness matrix also diagonalizes the damping rations matrix, is made:

$$[\tilde{\zeta}^*]=[\tilde{\Phi}]^T[\tilde{\zeta}][\tilde{\Phi}]=\begin{bmatrix}\tilde{\zeta}_1 & 0\\ 0 & \tilde{\zeta}_2\end{bmatrix} \tag{29}$$

where

$$\tilde{\zeta}_1=\tilde{\zeta}_{b11}-(1-\tilde{\alpha}_1)\left(\tilde{\zeta}_{b12}+\frac{\tilde{\zeta}_{s21}}{\tilde{R}_s}\right)+(1-\tilde{\alpha}_1)^2\left(\tilde{\zeta}_{b22}+\frac{1}{\tilde{R}_s}\tilde{\zeta}_{s22}\right) \tag{30}$$

$$\tilde{\zeta}_2=\tilde{\zeta}_{b11}-(1-\tilde{\alpha}_2)\left(\tilde{\zeta}_{b12}+\frac{\tilde{\zeta}_{s21}}{\tilde{R}_s}\right)+(1-\tilde{\alpha}_2)^2\left(\tilde{\zeta}_{b22}+\frac{1}{\tilde{R}_s}\tilde{\zeta}_{s22}\right) \tag{31}$$

Figs. 4–12 depict the effects of SSI on the response of a base-isolated building system. The structural (ζ_s) and isolation (ζ_b) viscous damping ratios are assumed to be equal to 2% and 25%, respectively. Also, the assumption that the structure exhibits elastic behaviour because the deformations develop primarily at the isolation level. The soil viscous damping ratio, ζ_g, is assumed to be equal to 5%, which implies small-to-moderate soil deformation levels. Figs. 4 and 5 present the variation of the $\tilde{\omega}_1/\omega_s$ ratio with the dimensionless parameter $\bar{s}$, for different values of $\bar{m}$. From Figs. 4 and 5 it can be observed that increasing $\bar{m}$ results in smaller values of $\tilde{\omega}_s/\omega_s$. The parameter $\bar{m}$ is a measure of the structural inertia; for a given foundation and assuming that the soil mass density is practically the same for most applications, larger values of $\bar{m}$ imply greater structural mass, attributed to either more stories in the structure or a larger mass in each storey. Thus, the larger $\bar{m}$, the greater is the anticipated inertial interaction. The $\tilde{\omega}_s/\omega_s$ ratio decreases significantly for increasing $\bar{s}$. As expected, as the shear wave velocity of the subsoil decreases, the effects of SSI on the frequency characteristics of the system become more pronounced.

Fig. 6 presents the variation of $\tilde{\omega}_s/\omega_s$ with $\bar{m}$. Notice that for $\bar{s}$ equal to zero, the structural frequency is the same for the 4-DOF and equivalent 2-DOF system. Such a behaviour is anticipated, since for a rigid foundation, there is no influence of soil flexibility on the system response. From Figs. 4–6 it can be deduced that the effect of SSI on the frequency of the structure is greater for stiff structures with flexible soil strata. Also, SSI becomes more significant for small values of the parameter $\bar{h}$, that implies larger values of $\tilde{\zeta}_1$, and of the parameter $\bar{m}$, that implies smaller values of $\tilde{\omega}_s/\omega_s$. Such a behaviour is also anticipated, since $\bar{h}$ and $\bar{m}$ are also

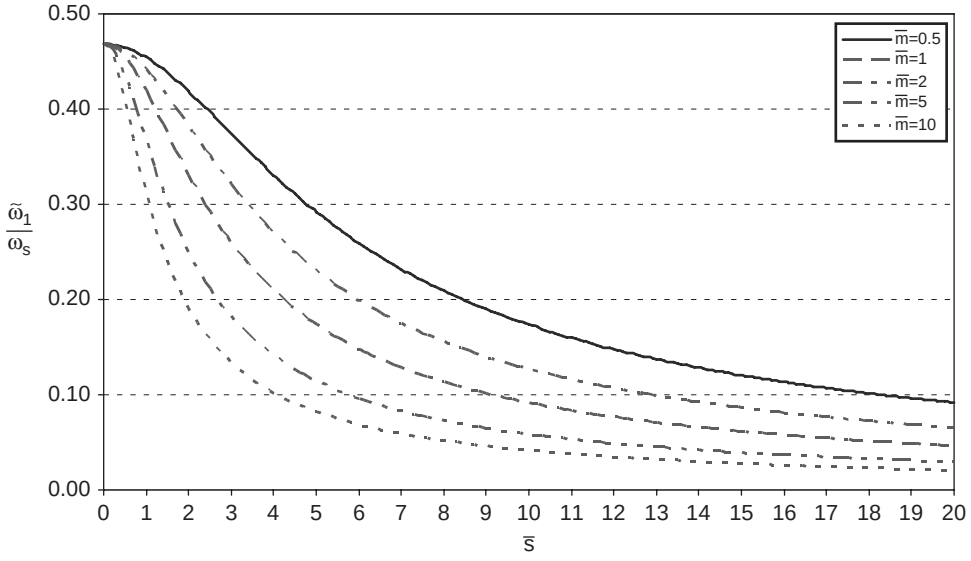

Fig. 4. Variation of frequency ratio $\tilde{\omega}_1/\omega_s$ for representative $\bar{m}$ ($\gamma=0.5$, $R_s=0.5$, $\nu=0.33$, $\bar{h}=1$, $\zeta_b=25\%$, $\zeta_s=2\%$, $\zeta_g=5\%$).

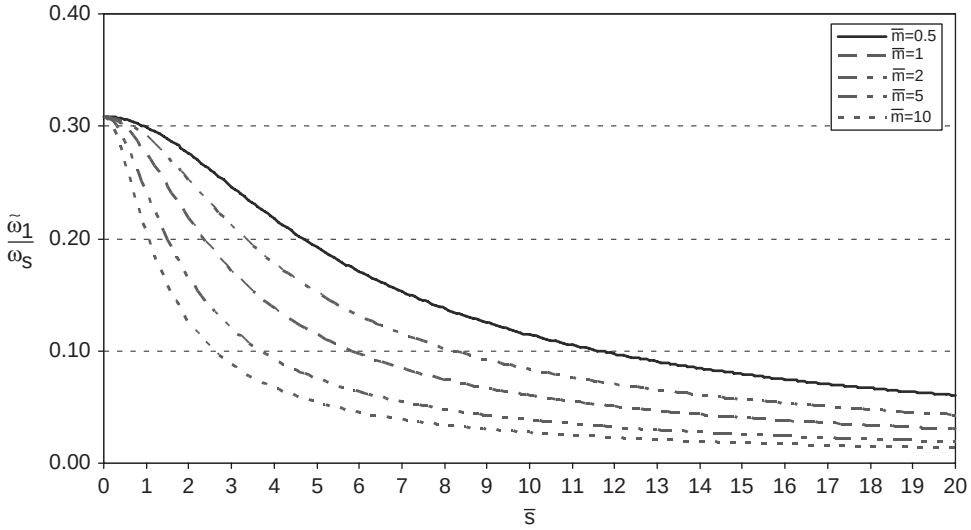

Fig. 5. Variation of frequency ratio $\tilde{\omega}_1/\omega_s$ for representative $\bar{m}$ ($\gamma = 0.5$, $R_s = 0.2$, $\nu = 0.33$, $\bar{h} = 1$, $\zeta_b = 25\%$, $\zeta_s = 2\%$, $\zeta_g = 5\%$).

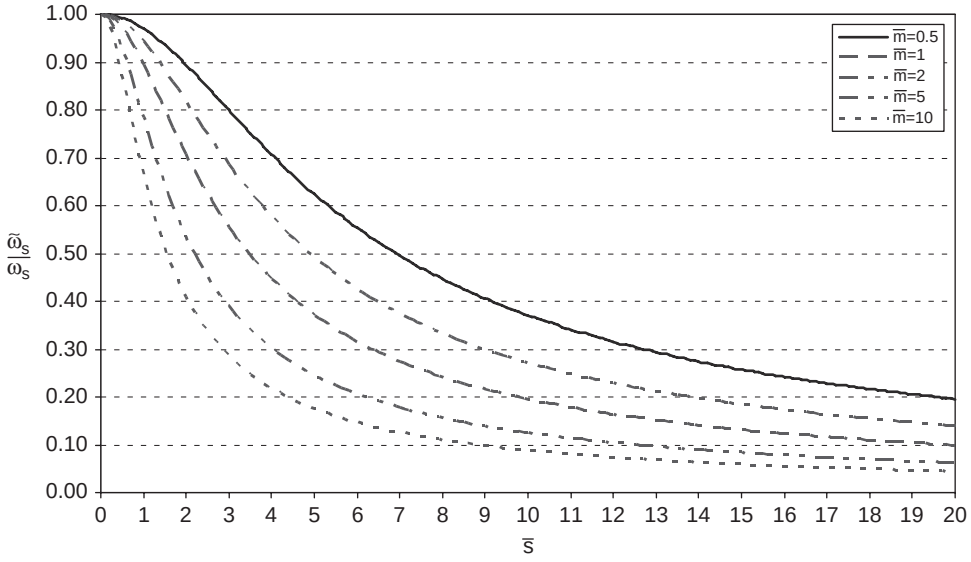

Fig. 6. Variation of frequency ratio $\tilde{\omega}_s/\omega_s$ for representative $\bar{m}$ ($\gamma = 0.5$, $R_s = 0.2$, $\nu = 0.33$, $\bar{h} = 1$, $\zeta_b = 25\%$, $\zeta_s = 2\%$, $\zeta_g = 5\%$).

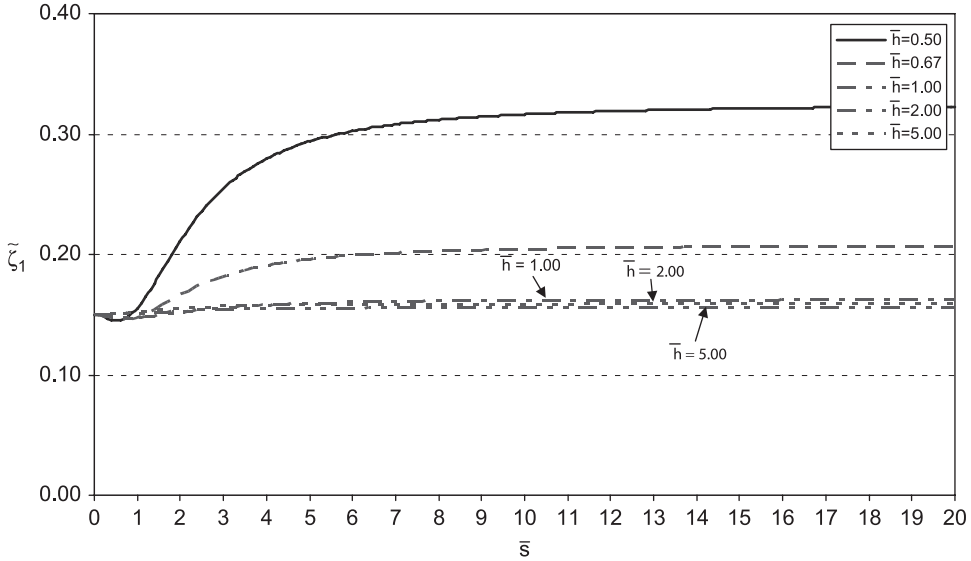

Fig. 7. Variation of composite damping ratio $\tilde{\zeta}_1$ for representative $\bar{h}$ ($\gamma = 0.5$, $R_s = 0.5$, $\nu = 0.33$, $\bar{m} = 3$, $\zeta_b = 25\%$, $\zeta_s = 2\%$, $\zeta_g = 5\%$).

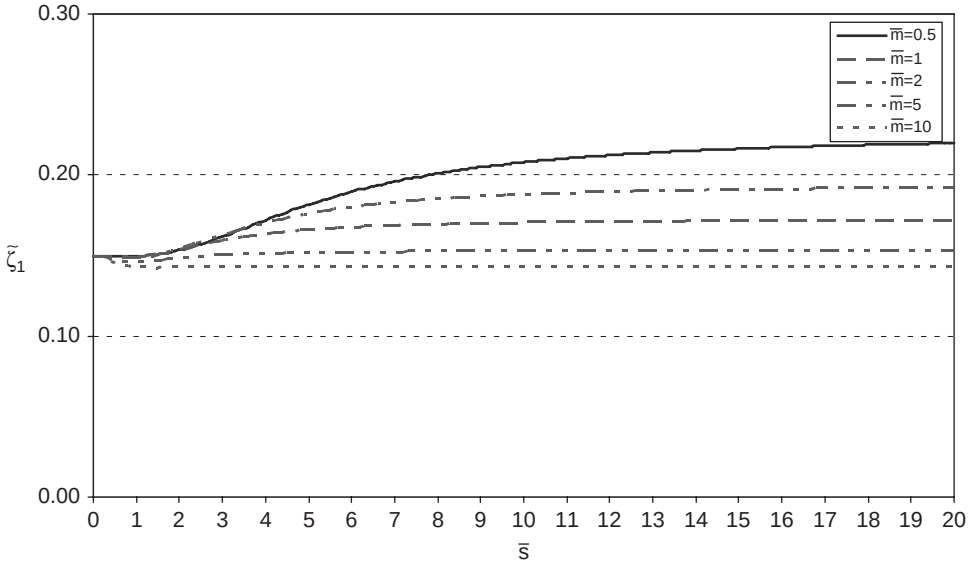

Fig. 8. Variation of composite damping ratio $\tilde{\zeta}_1$ for representative $\bar{m}$ ($\gamma = 0.5$, $R_s = 0.5$, $\nu = 0.33$, $\bar{h} = 1$, $\zeta_b = 25\%$, $\zeta_s = 2\%$, $\zeta_g = 5\%$).

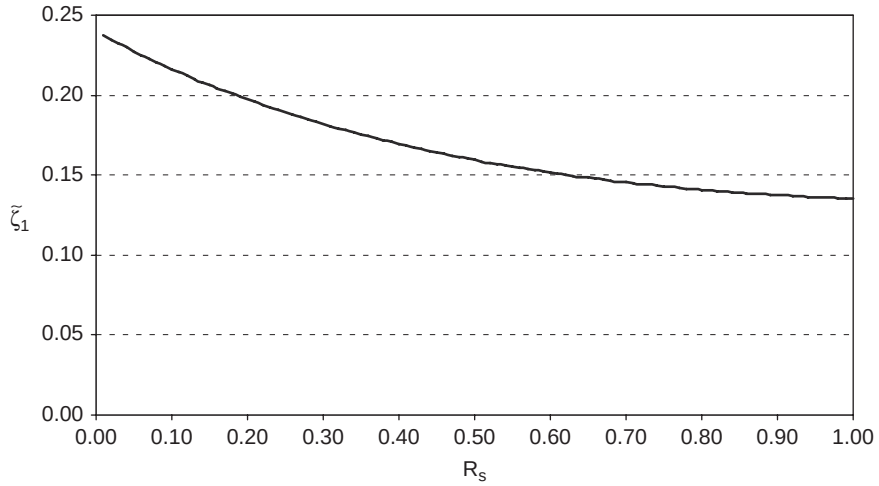

Fig. 9. Variation of composite damping ratio $\tilde{\zeta}_1$ with bearing-structure stiffness ratio, R_s ($\bar{s} = 5, m = 3, \bar{h} = 1$, $\gamma = 0.5$, $\zeta_b = 25\%$, $\zeta_s = 2\%$, $\zeta_g = 5\%$).

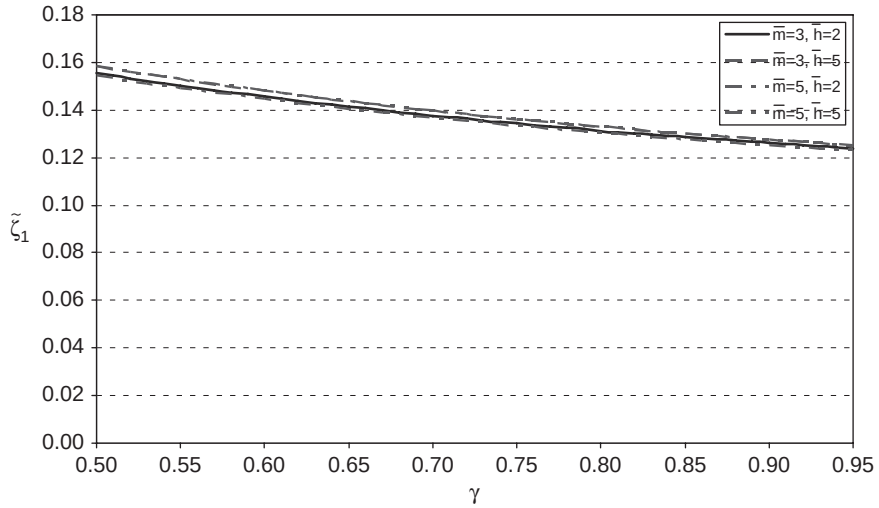

Fig. 10. Variation of composite damping ratio $\tilde{\zeta}_1$ with mass ratio, γ, for representative $\bar{m}$ and $\bar{h}$ ($\bar{s} = 5$, $R_s = 0.5$, $\nu = 0.33$, $\zeta_b = 25\%$, $\zeta_s = 2\%$, $\zeta_g = 5\%$).

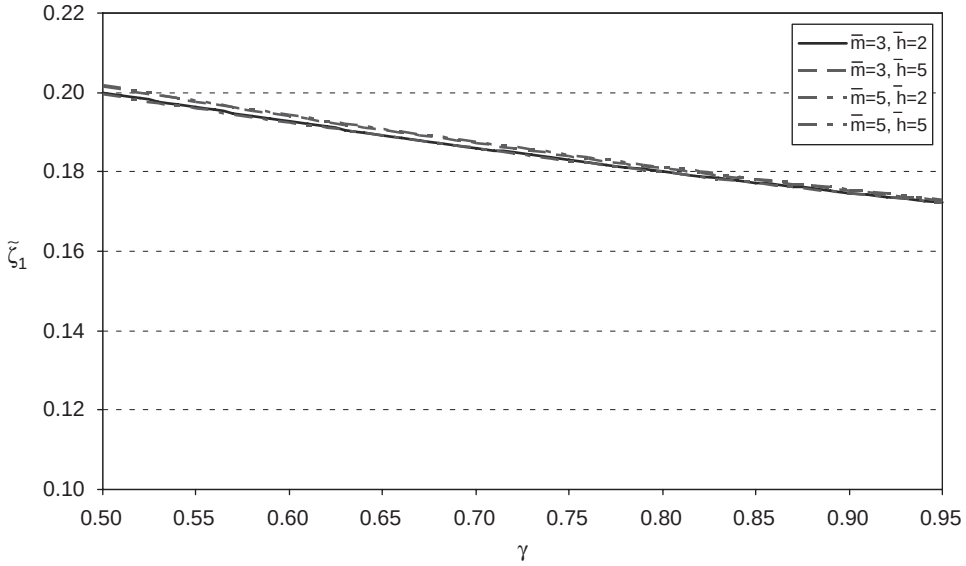

Fig. 11. Variation of composite damping ratio $\tilde{\zeta}_1$ with mass ratio, γ, for representative $\bar{m}$ and $\bar{h}$ ($\bar{s}=5$, $R_s=0.2$, $\nu=0.33$, $\zeta_b=25\%$, $\zeta_s=2\%$, $\zeta_g=5\%$).

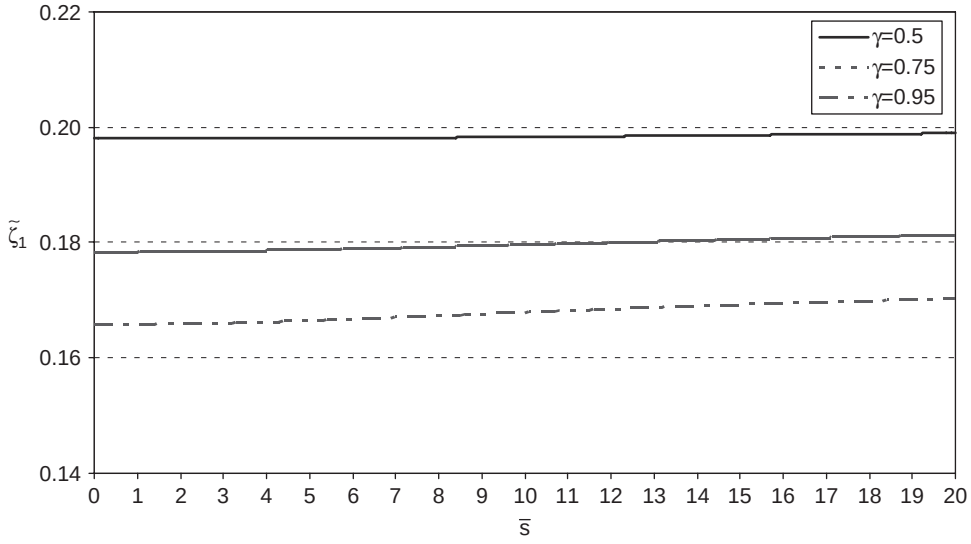

Fig. 12. Variation of composite damping ratio $\tilde{\zeta}_1$, for representative γ ($\bar{m}=3, \bar{h}=2$, $R_s=0.2$, $\nu=0.33$, $\zeta_b=25\%$, $\zeta_s=2\%$, $\zeta_g=5\%$).

measures of the relative structure–soil stiffness and inertia, respectively.

The variation of the soil–base isolation-structure system damping ratio, $\tilde{\zeta}_1$, with $\bar{s}$ for representative values of the parameters $\bar{h}$ and $\bar{m}$ is depicted in Figs. 7 and 8, respectively. It is observed that for a given value of $\bar{h}$ and $\bar{m}$, $\tilde{\zeta}_1$ increases with for decreasing structure–soil relative stiffness, expressed by an increase of the parameter $\bar{s}$. For $\bar{h}$ greater than 1, the composite damping ratio $\tilde{\zeta}_1$ is practically independent of $\bar{s}$. Also, as the mass ratio $\bar{m}$ increases, that is, for increasing structural inertia compared to the soil inertia, the effect of the relative stiffness of the soil $\bar{s}$ on affecting the composite damping ratio diminishes. With the exception of relatively squat structures of small height compared to the characteristic dimension of the foundation, i.e., $\bar{h}=0.5$ in Fig. 7, the influence of SSI on the equivalent damping ratio is not significant. The equivalent damping ratio of slender structures that display both translational and rocking deformations when excited, is not influenced by the relative soil stiffness, expressed by the parameter $\bar{s}$. From Fig. 8 it is observed that the effect of the dimensionless mass ratio $\bar{m}$ on the damping ratio of the equivalent system $\tilde{\zeta}_1$ is negligible for relatively stiff subsoil conditions, particularly for $\bar{s}$ values lower than 2, and becomes more significant for larger $\bar{s}$ values. Consequently, provided that the soil stiffness is relatively low, an increase in the structural mass expressed by the parameter $\bar{m}$ results in a decrease of the energy absorption capability of the equivalent system expressed by the composite damping ratio, $\tilde{\zeta}_1$.

The variation of $\tilde{\zeta}_1$ with R_s is presented in Fig. 9. This figure exhibits the influence of the relative stiffness between the structure and the isolation on the first modal damping ratio. An increase in the isolation system stiffness, while the structural stiffness is kept constant, results in a reduction of the composite damping ratio, caused by an increase in the structural deformation in the first mode of the isolation-structure system. For the limiting case of $R_s \to 1$ corresponding to a slender building structure that has similar stiffness with the isolation system, the

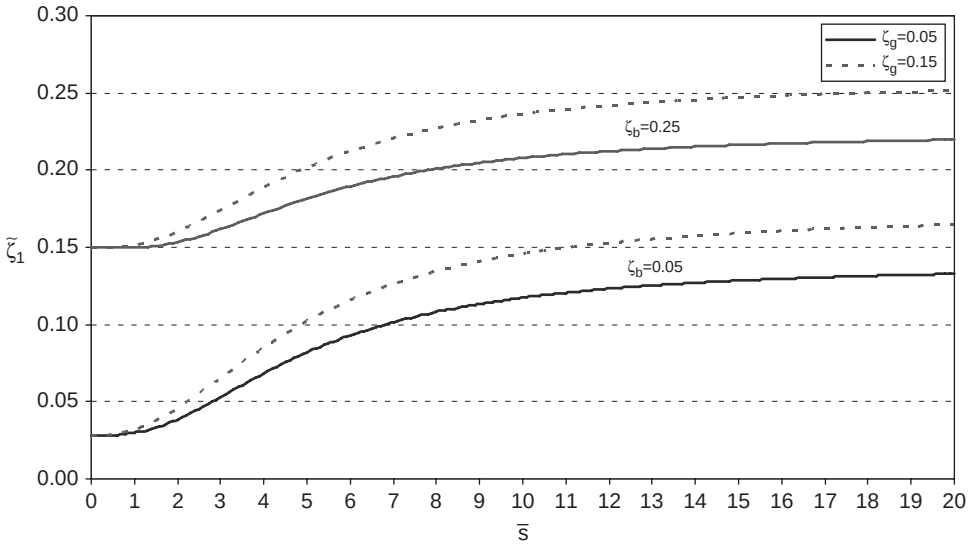

Fig. 13. Variation of composite damping ratio, $\tilde{\zeta}_1$, for representative ζ_b and ζ_g ($\bar{m}=0.5, \bar{h}=1$, $R_s=0.2$, $v=0.33$, $\zeta_s=2\%$).

decrease in damping is approximately 50%. Figs. 10–12 demonstrate the significance of the variation of the mass ratio γ on the composite damping ratio. The parameter γ defined in Eq. (3) expresses the relationship between the structural and isolation mass. The limiting case of $\gamma=0.5$ corresponds to a single story base-isolated building with the isolator mass that is the half of the total mass. Respectively, for the limiting case $\gamma\to 1.0$ the isolator mass should be considered as negligible compared with the structural mass, a case corresponding to a multi-storey building. Several values of the parameters $\bar{s}$, $\bar{m}$ and $\bar{h}$ have been considered and it appears that, independently from the relative mass and stiffness properties between the structure and soil, the influence of γ on $\tilde{\zeta}_1$ is rather small, compared to the influence of the other system parameters discussed previously, that is the mass ratio $\bar{m}$, the slenderness ratio $\bar{h}$ and the relative stiffness between the isolator and structure expressed by the parameter R_s. In Fig. 12 a value of the parameter $\gamma=0.75$ has also been considered, except for the limiting cases discussed previously, denoting an intermediate relation between m_s and m_b. In general, an increase in γ results in a decrease of the composite damping ratio.

Fig. 13 presents the variation of $\tilde{\zeta}_1$ with $\bar{s}$, for different values of the isolation system and soil half-space damping ratios, ζ_b and ζ_g, respectively. The influence of the isolation damping ratio on the composite damping ratio is larger than that of the soil damping ratios for small $\bar{s}$, since the response of the structure is primarily affected by the isolation mode. The influence of the soil damping ratio on the composite damping ratio is small, with the exception of very large $\bar{s}$. This behaviour may be attributed to the fact that base isolation leads to a more flexible structure that is less affected by SSI.

Based on the results of the parametric analysis, a preliminary assessment of the efficiency of base isolation on building structures can be made. Base isolation is more effective on light structures found on loose soil conditions. Alternatively, the characteristic length α should be selected greater than the structural height in order to result in small values of the mass and slenderness ratio. When multi-storey buildings are designed the increase of the structural mass compared to the isolator stiffness is not expected to be influential. An effort should be made to increase the structural stiffness relatively to the bearings stiffness, by either adding shear wall elements or using bearing elements of low horizontal stiffness. On loose soil conditions, use of natural rubber bearings of relatively small damping should be selected, while for stiff subsoil conditions, base isolators providing significant viscous damping such as lead rubber bearings should be used in order to provide sufficient energy absorption capability to the overall system. Regarding the combined effects of SSI and base isolation on the frequency characteristics of the system, an appropriate selection of the desirable increased period of the system should be made, based on the particular site characteristics. An increase of the structural period can be either destructive or beneficial accordingly to several parameters, such as the distance from a neighbouring fault, the type of the fault mechanism and the magnitude of the earthquake. It should be noted that a more elaborated analysis is necessary to provide insight in the response of a real three-dimensional base-isolated structure including SSI effects.

The results of the present investigation are limited to the range of relatively small frequency excitations, i.e., when the characteristic dimension of the footing is small compared with the wavelength of the excitation. For high frequency excitations, substantial changes on the modal characteristics of the system should be expected. According to Stewart et al. [32] a significant error can be introduced when neglecting the frequency dependence of the real part of the impedance function for structures with high modal frequency characteristics. In such a case a more accurate investigation should also include several significant factors affecting the overall response of the structure–foundation–soil system, such as: foundation shape, foundation mass, foundation flexibility or eccentricity effects, embedment and wave propagation effects.

3. Conclusions

The present work investigates the importance of SSI on the seismic response of base-isolated buildings founded on an elastic soil half-space. An equivalent 2-DOF fixed-base system is developed with frequency and damping parameters obtained from a 4-DOF system base-isolated building structure. The foundation stiffness and damping coefficients are assumed to be frequency-independent; however, frequency-dependent soil characteristics can be employed by simple modification of the derived expressions.

The results of the analysis and an extensive parametric study reveal the importance of SSI on the structure–base

isolation–foundation system frequency characteristics. The study demonstrates that the importance of SSI on the system damping is relatively small, the latter being greatly influenced by the base isolation system damping characteristics. It is also concluded that SSI effects are significant for relatively stiff, squat structures with small mass ratio $\bar{m}$. For preliminary design of base-isolated buildings, the methodology could serve as a means to assess the effects of SSI.

Acknowledgement

The research of Ch.A. Maniatakis is funded by a doctoral scholarship from the Alexander S. Onassis Public Benefit Foundation. This financial support is gratefully acknowledged.

Appendix A

Part I—Derivation of equivalent 2-DOF system equations

The equations of motion of the equivalent fixed-base 2-DOF system, shown in Fig. A1 and subjected to a harmonic base excitation $\tilde{u}_g e^{i\omega t}$, are:

$$-m_s\omega^2 u_s + i\omega\tilde{c}_s(u_s-u_b) + \tilde{k}_s(u_s-u_b) = m_s\omega^2\tilde{u}_g \tag{I.1}$$

$$-m_b\omega^2 u_b + i\omega\tilde{c}_b u_b - i\omega\tilde{c}_s(u_s-u_b) + \tilde{k}_b u_b - \tilde{k}_s(u_s-u_b) = m_b\omega^2\tilde{u}_g \tag{I.2}$$

By setting

$$\tilde{\zeta}_b = \frac{\omega\tilde{c}_b}{2\tilde{k}_b},\quad \tilde{\zeta}_s = \frac{\omega\tilde{c}_s}{2\tilde{k}_s},\quad \tilde{\omega}_b^2 = \frac{\tilde{k}_b}{m_b+m_s},\quad \tilde{\omega}_s^2 = \frac{\tilde{k}_s}{m_s} \tag{I.3}$$

Eqs. (I.1) and (I.2) can be written as

$$\left[1+2\tilde{\zeta}_s i - \frac{\omega^2}{\tilde{\omega}_s^2}\right]\tilde{u}_s - (1+2\tilde{\zeta}_s i)\tilde{u}_b = \frac{\omega^2}{\tilde{\omega}_s^2}\tilde{u}_g \tag{I.4}$$

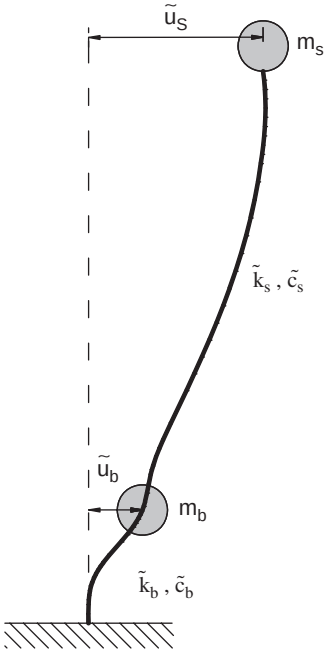

Fig. A1. Equivalent fixed-base 2-DOF system.

$$-\left[\frac{\tilde{\omega}_s^2}{\tilde{\omega}_b^2}\gamma(1+2\tilde{\zeta}_s i)\right]\tilde{u}_s + \left[1+2\tilde{\zeta}_b i + \frac{\tilde{\omega}_s^2}{\tilde{\omega}_b^2}\gamma(1+2\tilde{\zeta}_s i) - (1-\gamma)\frac{\omega^2}{\tilde{\omega}_b^2}\right] = (1-\gamma)\frac{\omega^2}{\tilde{\omega}_b^2}\tilde{u}_g \tag{I.5}$$

Eqs. (I.4) and (I.5) are equivalent to Eqs. (13) and (14).

Part II—Derivation of analytical expressions for equivalent 2-DOF system frequency and damping terms

Multiplying Eq. (7a) with γ and adding the resulting expression to Eq. (7b), results in:

$$-\gamma u_s + \left[-(1-\gamma) + \frac{\omega_b^2}{\omega^2}(1+2\zeta_b i)\right]u_b - u_o - \gamma h\varphi = u_g \tag{II.1}$$

Substituting Eq. (II.1) in Eqs. (7c) and (7d) and solving for u_o, yields

$$u_o = \left[\frac{\omega_b^2}{\omega^2}(1+2\zeta_b i)\right]u_b \frac{1}{\omega_h^2/\omega^2(1+2\zeta_h i+2\zeta_g i)} = \frac{\omega_b^2}{\omega_h^2}\frac{1+2\zeta_b i}{1+2\zeta_h i+2\zeta_g i}u_b \tag{II.2}$$

Equating the left-hand sides of Eqs. (7a) and (7d) leads to

$$h\varphi = \frac{\omega_s^2}{\omega_r^2}\frac{1+2\zeta_s i}{1+2\zeta_r i+2\zeta_g i}u_s - \frac{\omega_s^2}{\omega_r^2}\frac{1+2\zeta_s i}{1+2\zeta_r i+2\zeta_g i}u_b \tag{II.3}$$

Substituting Eqs. (II.2) and (II.3) into Eqs. (7a) and (7b), and performing a series of algebraic manipulations, yields

$$\left[\frac{\omega_s^2}{\omega^2}(1+2\zeta_s i) - \frac{\omega_s^2}{\omega_r^2}\frac{1+2\zeta_s i}{1+2\zeta_r i+2\zeta_g i} - 1\right]u_s + \left[-\frac{\omega_s^2}{\omega^2}(1+2\zeta_s i) + \frac{\omega_s^2}{\omega_r^2}\frac{1+2\zeta_s i}{1+2\zeta_r i+2\zeta_g i} - \frac{\omega_b^2}{\omega_r^2}\frac{1+2\zeta_b i}{1+2\zeta_h i+2\zeta_g i}\right]u_b = u_g \tag{II.4}$$

$$-\left[\frac{\omega_s^2}{\omega^2}\gamma(1+2\zeta_s i)\right]u_s + \left[-(1-\gamma) + \frac{\omega_b^2}{\omega^2}(1+2\zeta_b i) - (1-\gamma)\frac{\omega_b^2}{\omega_h^2}\frac{1+2\zeta_b i}{1+2\zeta_h i+2\zeta_g i} + \frac{\omega_s^2}{\omega^2}\gamma(1+2\zeta_s i)\right]u_b = (1-\gamma)u_g \tag{II.5}$$

Taking into account the fact that $(1)/(1+ai)\approx 1-ai$, for $a\ll 1$; neglecting the terms involving damping ratio products and multiplying both terms with ω^2/ω_s^2, Eq. (II.4) becomes

$$\left[1+2\zeta_s i - \frac{\omega^2}{\omega_r^2}(1+2\zeta_s i - 2\zeta_r i - 2\zeta_g i) - \frac{\omega^2}{\omega_s^2}\right]u_s + \left[-(1+2\zeta_s i) + \frac{\omega^2}{\omega_r^2}(1+2\zeta_s i - 2\zeta_r i - 2\zeta_g i) - \frac{\omega_b^2\omega^2}{\omega_h^2\omega_s^2}(1+2\zeta_b i - 2\zeta_h i - 2\zeta_g i)\right]u_b = \frac{\omega^2}{\omega_s^2}u_g \tag{II.6}$$

Applying the same procedure for Eq. (II.5) and multiplying both parts of the resulting expression with ω^2/ω_b^2, results in

$$\left[-(1-\gamma)\frac{\omega^2}{\omega_b^2} - (1-\gamma)\frac{\omega^2}{\omega_h^2}(1+2\zeta_b i - 2\zeta_h i - 2\zeta_g i) + (1+2\zeta_b i) + \frac{\omega_s^2}{\omega_b^2}\gamma(1+2\zeta_s i)\right]u_b - \left[\frac{\omega_s^2}{\omega_b^2}\gamma(1+2\zeta_s i)\right]u_s = (1-\gamma)\frac{\omega^2}{\omega_b^2}u_g \tag{II.7}$$

Eqs. (II.6) and (II.7) can be considered equivalent to Eqs. (I.4) and (I.5), respectively. The second parts of Eqs. (II.6) and (I.4) as

well as the coefficients of u_s and u_b are set equal, respectively:

$$\left[1+2\zeta_s i-\frac{\omega^2}{\omega_r^2}(1+2\zeta_s i-2\zeta_r i-2\zeta_g i)-\frac{\omega^2}{\omega_s^2}\right] = \left[1+2\tilde{\zeta}_{11} i-\frac{\omega^2}{\tilde{\omega}_s^2}\right] \tag{II.8}$$

$$\left[-(1+2\zeta_s i)+\frac{\omega^2}{\omega_r^2}(1+2\zeta_s i-2\zeta_r i-2\zeta_g i) -\frac{\omega_b^2\omega^2}{\omega_h^2\omega_s^2}(1+2\zeta_b i-2\zeta_h i-2\zeta_g i)\right] = -(1+2\tilde{\zeta}_{12} i) \tag{II.9}$$

$$\frac{\omega^2}{\omega_s^2}u_g=\frac{\omega^2}{\tilde{\omega}_s^2}\tilde{u}_g \tag{II.10}$$

Equating the real and imaginary parts in Eqs. (II.9) and (II.10) yields Eqs. (24a) and (24b) as well as the following expressions:

$$\frac{1}{\tilde{\omega}_s^2}=\frac{1}{\omega_s^2}+\frac{1}{\omega_r^2} \tag{II.11}$$

$$\frac{\omega^2}{\omega_r^2}-\frac{\omega^2\omega_b^2}{\omega_h^2\omega_s^2}=0 \tag{II.12}$$

Applying the same procedure for Eqs. (II.7) and (I.5) results in Eqs. (24c) and (24d) and the expressions

$$\frac{\omega_s^2}{\omega_b^2}=\frac{\tilde{\omega}_s^2}{\tilde{\omega}_b^2} \tag{II.13}$$

$$\frac{1}{\tilde{\omega}_b^2}=\frac{1}{\omega_b^2}+\frac{1}{\omega_h^2} \tag{II.14}$$

Eqs. (II.11) and (II.14) yield Eqs. (21) and (22) respectively,

References

[1] Wong HL, Luco JE. Dynamic response of rigid foundations of arbitrary shape. Earthquake Eng Struct Dyn 1976;4:587–97.
[2] Idriss IM, Kennedy RP, Agrawal PK, Hadjian AH, Kausel E, Lysmer J, et al. Analyses for soil–structure interaction effects for nuclear power plants. New York: ASCE; 1979.
[3] Spyrakos CC, Beskos DE. Dynamic response of flexible strip-foundations by boundary and finite elements. Soil Dyn Earthquake Eng 1986;5(2):84–96.
[4] Gazetas G. Foundation vibrations. In: Fang HY, editor. Foundation engineering handbook. 2nd ed. London: Chapman & Hall; 1991 (Chapter 15).
[5] Wolf JP. Dynamic soil–structure interaction. New Jersey: Prentice-Hall; 1985.
[6] Wolf JP. Foundation vibration analysis using simple physical models. New Jersey: Prentice-Hall; 1994.
[7] Goyal A, Chopra AK. Earthquake analysis of intake-outlet towers including tower–water–foundation–soil interaction. Earthquake Eng Struct Dyn 1989; 18:325–44.
[8] Xu C, Spyrakos CC. Seismic analysis of towers including foundation uplift. Eng Struct 1996;18(4):271–8.
[9] Maekawa K, Pimanmas A, Okamoura H. Nonlinear mechanics of reinforced concrete. London: Spon Press; 2003.
[10] Johnson JJ. Soil–structure interaction. In: Chen WF, Scawthorn C, editors. Earthquake engineering handbook, Part 2. Boca Raton, FL: CRC Press; 2003.
[11] FEMA 450. NEHRP recommended provisions for seismic regulations for new buildings and other structures (2003 edition). Building Seismic Safety Council (BSSC), Washington DC.
[12] Spyrakos CC. Soil–structure interaction in practice. In: Hall WS, Oliveto G, editors. Boundary element methods for soil–structure interaction. Dordrecht: Kluwer Academic Publishers; 2003 (Chapter 5).
[13] Naeim F, Kelly JM. Design of seismic isolated structures—from theory to practice. New York: Wiley; 1999.
[14] Komodromos P. Seismic isolation for earthquake resistant structures. Southampton: WIT Press; 2000.
[15] Skinner RI, Robinson WH, McVerry GH. An introduction to seismic isolation. Chichester: Wiley; 1993.
[16] Chopra AK. Dynamics of structures: theory and applications to earthquake engineering. 2nd ed. New Jersey: Prentice-Hall; 2001.
[17] International Code Council (ICC). International Building Code (IBC), Falls Church, VA, 2000.
[18] Eurocode 8, Design of structures for earthquake resistance-EN 1998 (2004 edition). European committee for standardization (CEN). Brussels.
[19] Chaudhary MTA, Abé M, Fujino Y. Identification of soil–structure interaction effect in base-isolated bridges from earthquake records. Soil Dyn Earthquake Eng 2001;21(8):713–25.
[20] Spyrakos CC, Vlassis AG. Effect of soil–structure interaction on seismically isolated bridges. J Earthquake Eng 2002;6(3):391–429.
[21] Vlassis AG, Spyrakos CC. Seismically isolated bridge piers on shallow soil stratum with soil–structure interaction. Comput Struct 2001;79(32): 2847–61.
[22] Sarrazin M, Moroni O, Roesset JM. Evaluation of dynamic response characteristics of seismically isolated bridges in Chile. Earthquake Eng Struct Dyn 2005;34(4–5):425–38.
[23] Iemura H, Pradono MH. Passive and semi-active seismic response control of a cable-stayed bridge. J Struct Control 2002;9(3):189–204.
[24] Tongaonkar NP, Jangid RS. Seismic response of isolated bridges with soil–structure interaction. Soil Dyn Earthquake Eng 2003;23(4):287–302.
[25] Cho KH, Kim MK, Lim YM, Cho SY. Seismic response of base-isolated liquid storage tanks considering fluid–structure–soil interaction in time domain. Soil Dyn Earthquake Eng 2004;24(11):839–52.
[26] Kim MK, Lin YM, Cho SY, Cho KH, Lee KW. Seismic analysis of base-isolated liquid storage tanks using the BE–FE–BE coupling technique. Soil Dyn Earthquake Eng 2002;22(9–12):1151–8.
[27] Constantinou MC, Kneifati MC. Effect of soil–structure interaction on damping and frequencies of base-isolated structures. In: Proceedings of third US national conference on earthquake engineering, vol. I. Charleston 1986.
[28] Tsai CS, Chen CS, Chen BJ. Effects of unbounded media on seismic responses of FPS-isolated structures. Struct Control Health Monit 2004; 11(1):1–20.
[29] Priestley MJN. Myths and fallacies in earthquake engineering, revisited. The Mallet Milne lecture. Pavia: Rose School; 2003.
[30] Antes H, Spyrakos CC. Soil–structure interaction. In: Beskos DE, Anagnostopoulos SA, editors. Computer analysis and design of earthquake resistant structures. Computational Mechanics Publications; 1997 (Chapter 6).
[31] Veletsos AS, Ventura CE. Modal analysis of non-classically damped systems. Earthquake Eng Struct Dyn 1986;14:217–43.
[32] Stewart JP, Seed RB, Fenves GL. Empirical evaluation of inertial soil–structure interaction effects. Report no. PEER-98/07, 1998.